# Appendix

## Appendix Table of Contents

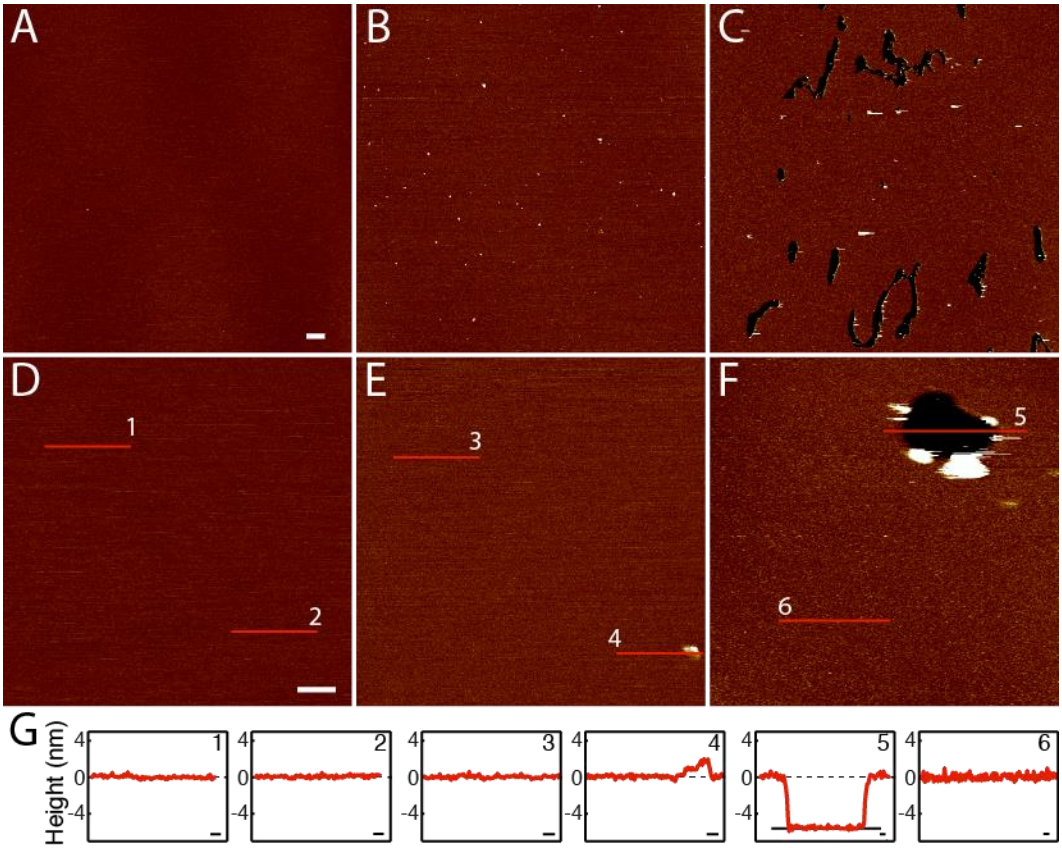


**Appendix Figure S1. Characterization of the supported lipid membrane (SLM) by AFM imaging.**

(A) AFM topograph of freshly cleaved atomically flat muscovite mica.

(B) Topograph of SLM made from *E. coli* polar lipid extract and uniformly covering the supporting mica.

(C) Topograph recorded of SLM made from *E. coli* polar lipid extract after air drying for 1 min. Holes and cracks of the SLM (black areas) are observed.

(D, E) Topographs of SLM made from *E. coli* polar lipid extract and uniformly covering the supporting mica.

(F) Topograph recorded of SLM made from *E. coli* polar lipid extract after air drying for 1 min. Holes and cracks of the SLM (black areas) are observed.

(G) Height profiles measured along the red lines indicated in AFM topographs (D-F). The black thick line in (5) indicates the mica surface at ≈ –5 nm height and the black dashed lines indicate the SLM surface at ≈ 0 nm height in (4, 5).

All AFM topographs were recorded in buffer solution at room temperature (Materials and Methods). The full color range of the topographs corresponds to a vertical scale of 5 nm. Scale bars, 1 µm (A-C) and 50 nm (D-F).

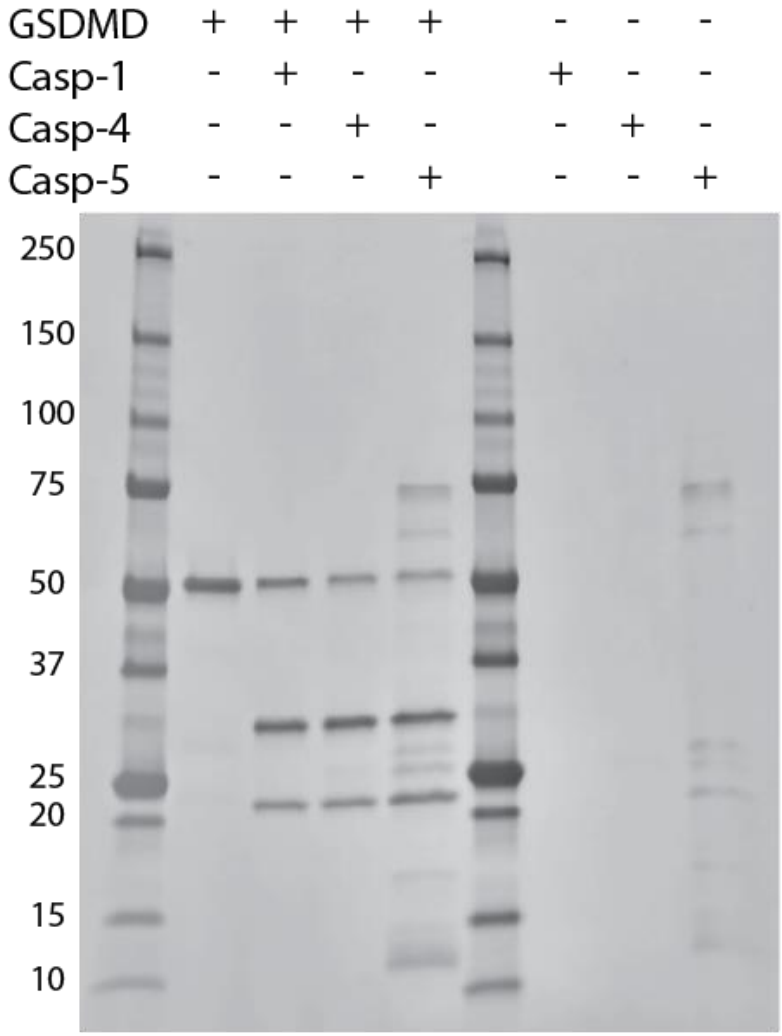


**Appendix Figure S2. GSDMD is cleaved by three different caspases to the same fragments**.

SDS-PAGE analysis of a protease cleavage reaction of 2 µM human GSDMD cleaved with either 5 nM caspase-1, -4, or -5 (Casp-1, Casp-4, Casp-5). Cleavage of the 53 kDa large GSDMD results in two fragments of 31 kDa ($GSDMD^{Nterm}$) and 22 kDa ($GSDMD^{Cterm}$). Molecular weight markers (in kDa) are annotated. Note that the caspase-5 sample contains trace impurities, which do not affect the cleavage reaction.

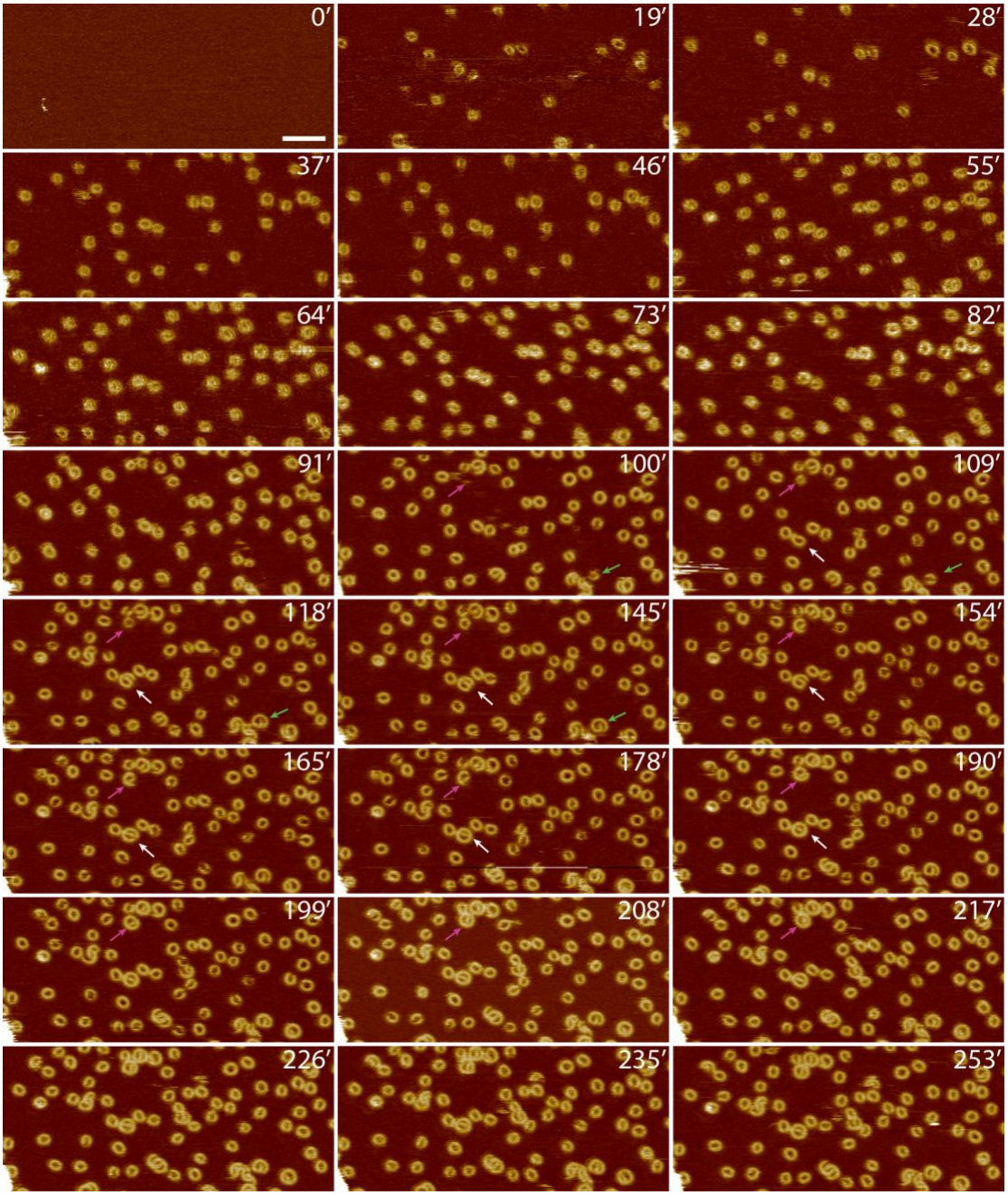


**Appendix Figure S3. Additional time-lapse AFM of GSDMD$^{Nterm}$ oligomerization and pore formation.**

The first FD-based AFM topograph of a SLM made from POPC, DOPG, DOPS, DOPE, and CL (40:20:10:20:10 molar ratio) was used as a control to show that the lipid membrane was defect-free. The defect-free SLM was then incubated with GSDMD and caspase-1 in buffer solution at 37°C. Recorded at different time points of the incubation (indicated by time stamps in min) the time-lapse topographs follow the progress of GSDMD$^{Nterm}$ binding and assembly to the SLM. Arrows indicate examples of GSDMD$^{Nterm}$ arc- or slit-shaped oligomers that grow into larger ring-shaped oligomers. The full color range of the topographs corresponds to a vertical scale of 10 nm. Scale bar, 50 nm.

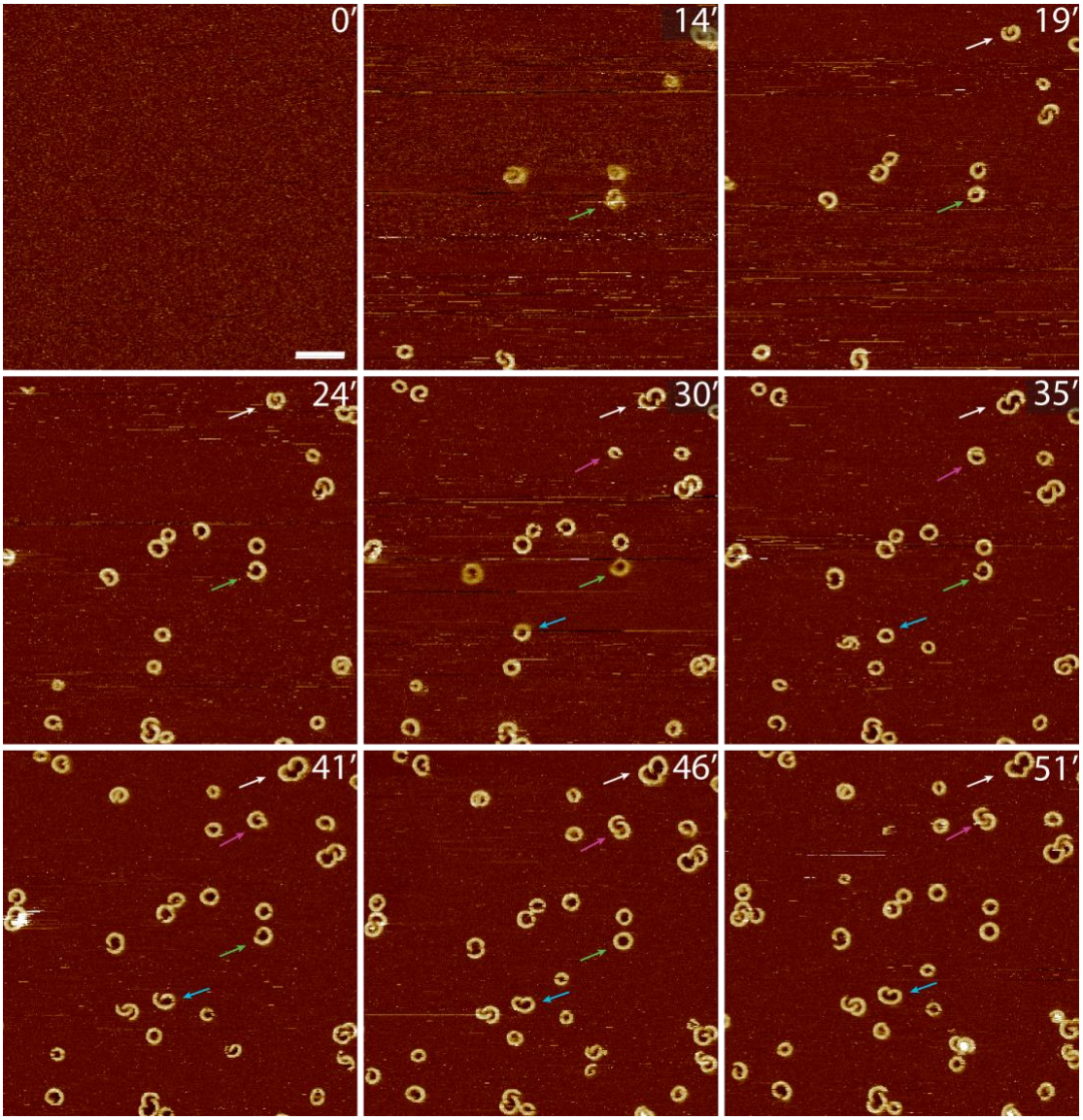


**Appendix Figure S4. Additional time-lapse AFM of GSDMD$^{Nterm}$ oligomerization and pore formation.**

The first FD-based AFM topograph of a SLM made from POPC, DOPG, DOPS, DOPE, and CL (40:20:10:20:10 molar ratio) was used as a control to show that the SLM was defect-free. The defect-free SLM was then incubated with GSDMD and caspase-1 in buffer solution at 37°C. Recorded at different time points of the incubation (indicated by time stamps in min) the time-lapse topographs follow the progress of GSDMD$^{Nterm}$ binding and assembly to the SLM. Arrows indicate examples of GSDMD$^{Nterm}$ oligomers growing into larger oligomers. The full color range of the topographs corresponds to a vertical scale of 10 nm. Scale bar, 100 nm.

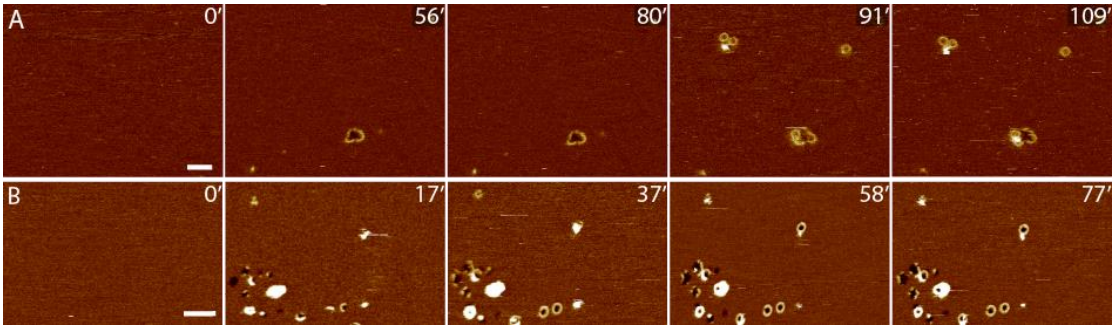


**Appendix Figure S5. Time-lapse topographs of GSDMD$^{Nterm}$ oligomerization and pore formation in SLMs made from POPG and POPC.**

The first AFM topographs at the left show SLMs made from (A) POPG or (B) POPC before of their incubation with GSDMD and caspase-1. The following AFM topographs show the SLMs incubated with GSDMD and caspase-1 buffer solution at 37°C. In each topograph the time point of the incubation is indicated by the time stamp (in min). The time-lapse FD-based AFM topographs were recorded in buffer solution at 37°C as described (**Materials and Methods**). The full color range of the topographs corresponds to a vertical scale of 10 nm. Scale bars, 50 nm

| SLM | Slit-shaped oligomers Height above SLM (mean ± SE) | Ring-shaped oligomers Height above SLM (mean ± SE) | Ring-shaped oligomers Diameter (mean ± SE) |
|---|---|---|---|
| POPC, DOPG, DOPS, DOPE, and CL (40:20:10:20:10 molar ratio) | 3.6 ± 0.2 nm<br>(*n* = 74) | 3.6 ± 0.3 nm<br>(*n* = 277) | 22.6 ± 0.3 nm<br>(*n* = 288) |
| *E. coli* polar lipid extract | 3.5 ± 0.3 nm*<br>(*n* = 135)<br>*P* = 0.01 | 3.5 ± 0.3 nm$^{NS}$<br>(*n* = 164)<br>*P* = 0.08 | 23.1 ± 0.7 nm$^{NS}$<br>(*n* = 183)<br>*P* = 0.32 |
| *E. coli* polar lipid extract and cholesterol (70:30 weight ratio) | 3.5 ± 0.3 nm$^{NS}$<br>(*n* = 35)<br>*P* = 0.09 | 3.4 ± 0.4 nm*<br>(*n* = 63)<br>*P* = 0.008 | 21.2 ± 0.4 nm*<br>(*n* = 94)<br>*P* = 0.001 |
| POPS, DOPE and POPC (35:25:40 molar ratio) | 3.2 ± 0.2 nm*<br>(*n* = 23)<br>*P* = 1.8 $10^{-12}$ | 3.3 ± 0.2 nm*<br>(*n* = 20)<br>*P* = 3.0 $10^{-5}$ | 25.8 ± 1.6 nm$^{NS}$<br>(*n* = 20)<br>*P* = 0.06 |
| POPS, DOPE and PI(4,5)P2 (35:25:40 molar ratio) | 3.2 ± 0.3 nm*<br>(*n* = 53)<br>*P* = 3.0 $10^{-5}$ | 3.2 ± 0.2 nm*<br>(*n* = 70)<br>*P* = 2.0 $10^{-23}$ | 26.7 ± 0.5 nm*<br>(*n* = 112)<br>*P* = 9.0 $10^{-5}$ |

**Appendix Table S1. Characterization of slit- and ring-shaped GSDMD$^{Nterm}$ oligomers formed in SLM made from different lipid compositions and imaged by AFM.**
Statistical significances were calculated using a two-tailed T-test comparing oligomeric heights relative to the POPC, DOPG, DOPS, DOPE, and CL (40:20:10:20:10 molar ratio) condition. Values were considered significant * if $P < 0.05$ and non-significant (*NS*) if $P \geq 0.05$. FD-based AFM imaging was conducted as described in the main manuscript and **Materials and Methods**.

| Caspase | Slit-shaped oligomers Height above SLM (mean ± SE) | Ring shaped oligomers Height above SLM (mean ± SE) | Ring shaped oligomers Diameter (mean ± SE) |
|---|---|---|---|
| GSDMD-caspase-1 | 3.6 ± 0.2 nm<br>(*n* = 74) | 3.6 ± 0.3 nm<br>(*n* = 277) | 22.6 ± 0.3 nm<br>(*n* = 288) |
| GSDMD-caspase-4 | 3.3 ± 0.2 nm*<br>(*n* = 38)<br>*P* = 1.0 $10^{-9}$ | 3.4 ± 0.3 nm*<br>(*n* = 196)<br>*P* = 1.0 $10^{-11}$ | 25.1 ± 0.2 nm*<br>(*n*=230)<br>*P* = 5.0 $10^{-11}$ |
| GSDMD-caspase-5 | 3.5± 0.4 nm*NS*<br>(*n* = 41)<br>*P* = 0.1 | 3.5 ± 0.4 nm*<br>(*n* = 115)<br>*P* = 0.02 | 25.0 ± 0.1 nm*<br>(*n*=169)<br>*P* = 1.0 $10^{-12}$ |

**Appendix Table S2. Characterization of slit- and ring-shaped GSDMD$^{Nterm}$ oligomers imaged by AFM after cleavage of GSDMD by either caspase-1, -4 or -5.**
GSDMD$^{Nterm}$ oligomers were imaged in SLMs made from POPC, DOPG, DOPS, DOPE, and CL (40:20:10:20:10 molar ratio). Statistical significances were calculated using a two-tailed T-test comparing oligomeric heights relative to the caspase-1 condition. Values were considered significant * if $P < 0.05$ and non-significant (*NS*) if $P \geq 0.05$. FD-based AFM imaging was conducted as described in the main manuscript and **Materials and Methods**.

| Lipid membrane composition | Data shown in | Membrane Binding | Assembly in arc-, slit- and ring-like oligomers | Pore formation |
|---|---|---|---|---|
| POPC, DOPG, DOPS, DOPE, and CL (40:20:10:20:10 molar ratio) | Fig. 1, Fig. 3, Fig. 4, Fig. 5, Fig. EV5 Appendix Fig. S3, Appendix Fig. S4, | Yes | Yes | Yes |
| *E. coli* polar lipid extract | Fig. 1, Fig. EV3 | Yes | Yes | Yes |
| *E. coli* polar lipid extract and cholesterol (70:30 weight ratio) | Fig. 1 | Yes, reduced | Yes | Yes |
| POPS, DOPE and POPC (35:25:40 molar ratio) | Fig. 2 | Yes | Yes | Yes |
| POPS, DOPE and POPI (35:25:40 molar ratio) | Fig. 2 | No | No | No |
| POPS, DOPE and PI(4,5)P2 (35:25:40 molar ratio) | Fig. 2 | Yes | Yes | Yes |
| POPS, POPC, DOPE and PI(4,5)P2 (35:30:25:10 molar ratio) | Fig. EV4 | Yes | Yes | Yes |
| POPS, POPC, DOPE, PI(4,5)P2 and cholesterol (30:26:21:8:15 molar ratio) | Fig. EV4 | Yes, reduced | Yes | Yes |
| POPS, POPC, DOPE, PI(4,5)P2 and cholesterol (24:21:18:7:30 molar ratio) | Fig. EV4 | Largely suppressed | No | No |
| POPG | Appendix Fig. S5 | Yes, reduced | Yes | Yes |
| POPC | Appendix Fig. S5 | Yes, reduced | Yes | Yes |

**Appendix Table S3. Summary of lipid membrane compositions tested to characterize GSDMD$^{Nterm}$ binding, oligomerization and pore formation.**